Product Datasheet

PINK1 Antibody - BSA Free
BC100-494SS

Unit Size: 0.025 ml

Store at 4C short term. Aliquot and store at -20C long term. Avoid freeze-thaw cycles.

www.novusbio.com technical@novusbio.com

Reviews: 13 Publications: 274

Protocols, Publications, Related Products, Reviews, Research Tools and Images at:
www.novusbio.com/BC100-494

Updated 12/20/2023 v.20.1

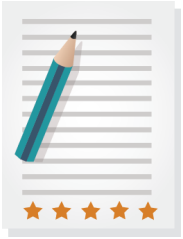

BC100-494SS

PINK1 Antibody - BSA Free

Product Information	
Unit Size	0.025 ml
Concentration	1.0 mg/ml
Storage	Store at 4C short term. Aliquot and store at -20C long term. Avoid freeze-thaw cycles.
Clonality	Polyclonal
Preservative	0.02% Sodium Azide
Isotype	IgG
Purity	Immunogen affinity purified
Buffer	PBS
Target Molecular Weight	62.7 kDa

Product Description	
Host	Rabbit
Gene ID	65018
Gene Symbol	PINK1
Species	Human, Mouse, Rat, Rabbit
Reactivity Notes	Use in Mouse reported in scientific literature (PMID:33775690). All species in which poly(GP) peptides are synthesized. Human reactivity reported in multiple pieces of scientific literature.
Specificity/Sensitivity	Human PINK1 Antibody will be reactive to isoform 2.
Immunogen	PINK1 antibody was developed using a synthetic peptide made to the human PINK1 protein sequence (between residues 175-250). [Swiss-Prot Q9BXM7]

Product Application Details	
Applications	Western Blot, Electron Microscopy, Immunoblotting, Immunocytochemistry/ Immunofluorescence, Immunohistochemistry, Immunohistochemistry-Frozen, Immunohistochemistry-Paraffin, Immunoprecipitation, SDS-Page, Peptide ELISA, Knockdown Validated, Knockout Validated
Recommended Dilutions	Western Blot 1:500 - 1:2000, Immunohistochemistry, Immunocytochemistry/ Immunofluorescence 1:50 - 1:200, Immunoprecipitation reported in scientific literature (PMID 22078885), Immunohistochemistry-Paraffin reported in scientific literature (PMID 25083992), Immunohistochemistry-Frozen reported in scientific literature (PMID 31908016), Immunoblotting reported in multiple pieces of scientific literature, Peptide ELISA 1:100 - 1:2000, Electron Microscopy, SDS-Page reported in scientific literature (PMID 27846363), Knockout Validated reported in scientific literature (PMID 31066324), Knockdown Validated
Application Notes	NOTE: It's recomended to use 1-5% w/v BSA in TBS with 0.1% Tween-20 for all incubations in WB. Specific bands are seen at 48, 55 and 63 kDa in Western Blot. In WB, this antibody has been used in valinomycin and CCCP treated HeLa whole cell lysate.

Images

PINK1/Parkin-mediated mitophagy. Western Blot of mitochondrial and cytosolic fractions for PINK1, Parkin, and ubiquitin. E Quantitation of protein levels, normalized to VDAC and GAPDH, Ubiquitin: n = 6, PINK1: n = 5, Parkin: n = 8. R, post-reoxygenation. Image collected and cropped by CiteAb from the following publication (//pubmed.ncbi.nlm.nih.gov/33980811/) licensed under a CC-BY license.

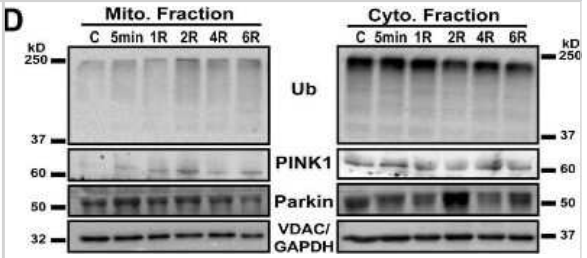

Immunocytochemistry of PINK1 antibody (BC100-494 Lot G). HeLa cells were treated with valinomycin (1 uM for 24h) prior to being fixed in 10% buffered formalin for 10 min and permeabilized in 0.1% Triton X-100 in PBS for 10 min. Cells were incubated with BC100-494 at 20 ug/mL for 1h at room temperature, washed 3x in PBS and incubated with Alexa Fluor488 anti-rabbit secondary antibody. PINK1 (Green) was detected at the mitochondria. Tubulin (Red) was detected using an anti-tubulin antibody with an anti-mouse DyLight 550 secondary antibody. DNA (Blue) was counterstained with DAPI. Note: mitochondria staining might not be easily observed without treatment with valinomycin or CCCP.

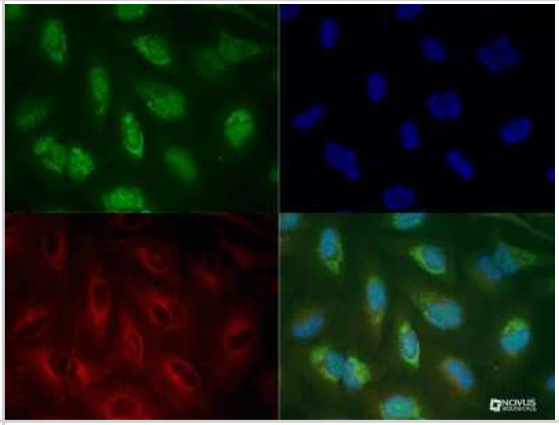

Confocal microscopy analysis of the mitophagy initiation in the RPE cells by staining PINK1 and PARKIN. One-year-old WT and dKO mice focusing on the RPE cells in the vicinity of the optic nerve (a,e). PINK1 (b, red) and PARKIN (c, green) were double-stained and the merged image (d) was used to count the colocalized puncta from WT. Similarly, in dKO PINK1 (f, red) and PARKIN (g, green) were double-stained, and the merged image (h) was used to count the colocalized puncta. dKO = NFE2L2/PGC1a double knockout. Image collected and cropped by CiteAb from the following publication (//pubmed.ncbi.nlm.nih.gov/32183173/) licensed under a CC-BY license.

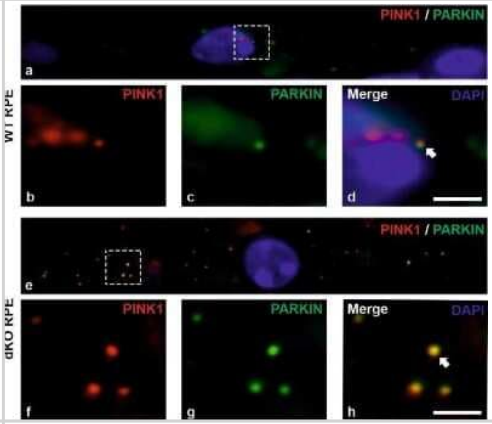

Western blot image of PINK1 antibody (BC100-494) in multiple cells lines. Human HeLa (lane 1), Mouse NIH-3T3 (lane 2), L929 (lane 3) and Rat PC12 (lane 4) whole cell protein were separated by SDS-PAGE on a 7.5% polyacrylamide gel. Protein was transferred to PVDF membrane and probed with 2 ug/mL BC100-494 in 1% BSA and detected with an HRP-conjugated anti-rabbit secondary antibody using chemiluminescence. Observed molecular weight ~55 kDa (arrowhead).

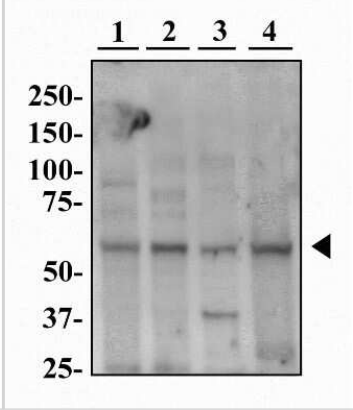

Analysis of PINK1 in mouse liver and hypatocytes using PINK1 antibody. Observed molecular weight ~55 kDa. WB image submitted by a verified customer review.	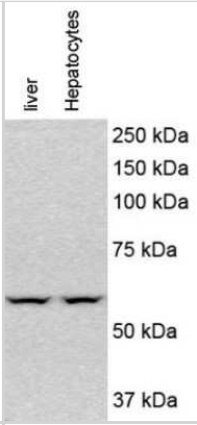
Pathogenic mutants of Parkin are subjected to Ser65 phosphorylation. Phos-tag Western blotting for Parkin and Western blotting for PINK1 were performed using Parkin WT and a series of pathogenic mutants. Image collected and cropped by CiteAb from the following publication (https://www.nature.com/articles/srep01002) licensed under a CC-BY license.	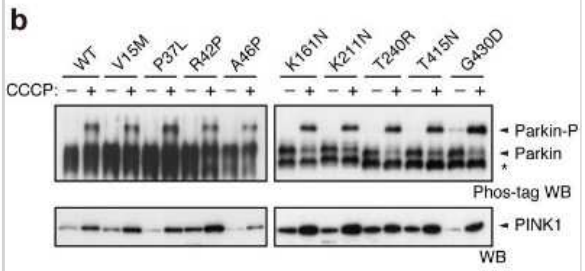
Alteration of mitochondria and PD associated proteins in SH-SY5Y cells with telomere removal by CRISPR-Cas9. Representative Western blot of PGC-1alpha, NRF1, and PINK1 in SH-SY5Y cells transfected with either gTel or gCont (72 h). Beta-actin served as a loading control. Image collected and cropped by CiteAb from the following publication (https://www.mdpi.com/1422-0067/18/10/2093), licensed under a CC-BY license.	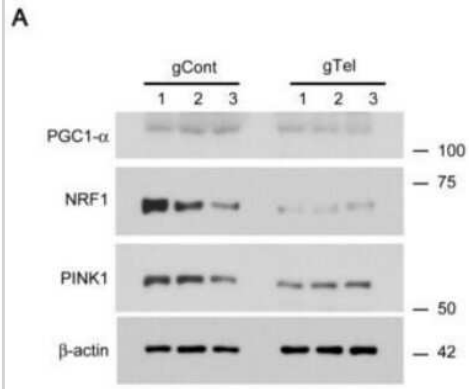
35 ug Neuro2A whole cell lysate separated on 8% PAGE and stained for PINK1 (1:1000 in 5% milk powder in TBST; secondary antibody AP at 1:5000). WB image submitted by a verified customer review.	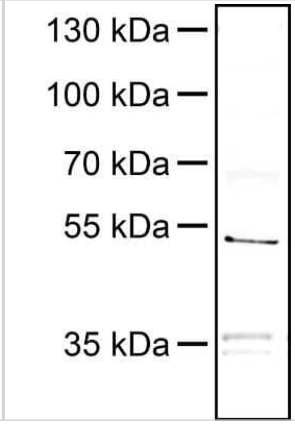

Rabbit heart tissue. IHC-P image submitted by a verified customer review.	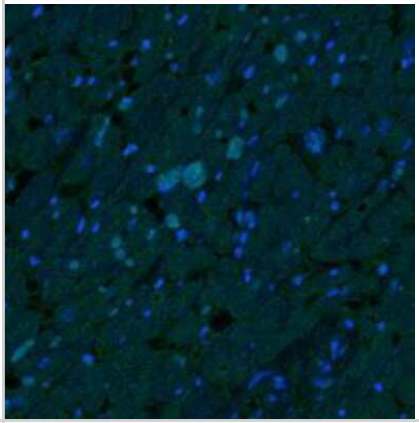
HEK293 cells were co-transfected with PINK1 siRNA (#1 or #2) or scrambled siRNA (scrambled) and untagged wild-type (WT) or Ser65Ala (S65A) mutant Parkin as indicated using TransFectin reagent (Bio-Rad). 48 hrs post-transfection, cells were treated with/without 10 uM CCCP for 3 h. 0.25 mg of 1% Triton whole-cell lysate were subjected to immunoprecipitation with GST-Parkin antibody (S966C) covalently coupled to protein G Sepharose and then immunoblotted with anti-phospho-Ser65 antibody in the presence of dephosphorylated peptide. 5% of the IP was immunoblotted with total anti-Parkin antibody. 0.25 mg of whole-cell lysates were immunoprecipitated with anti-PINK1 antibody (S085D) and immunoblotted with anti-PINK1 antibody. Representative of three independent experiments. Image collected and cropped by CiteAb from the following publication (https://rsob.royalsocietypublishing.org/cgi/doi/10.1098/rsob.120080) licensed under a CC-BY license.	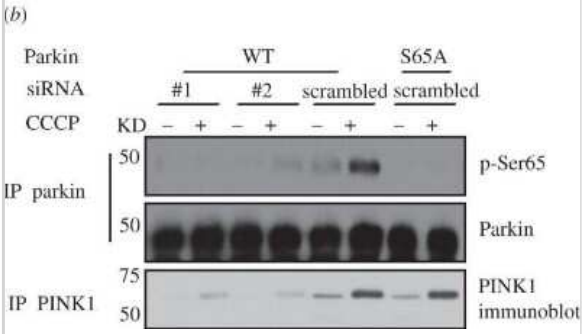
Characterisation of mitochondrial content and function in PINK1-/- platelets. Cropped immunoblots showing PINK1 expression in 10 uM CCCP (6 hours) treated WT, but not KO platelets by IP (upper panel) with loading control of IP inputs by blotting for PINK1 (lower panel). Uncropped blots for PINK1 are provided in Supplementary Fig. S1b. Image collected and cropped by CiteAb from the following publication (https://www.nature.com/articles/s41598-018-32716-4), licensed under a CC-BY license.	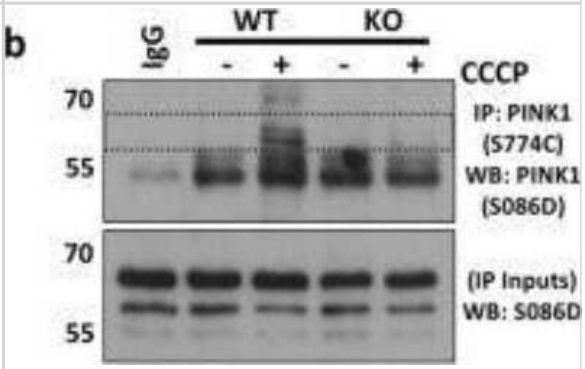
Representative TEM picture. The red and green arrows indicate PINK and PARKIN immunogold particles in the dKO RPE samples, respectively (e). ML, melanosome. Scale = 0.2 um. Mitochondria (M). Image collected and cropped by CiteAb from the following publication (https://pubmed.ncbi.nlm.nih.gov/32183173) licensed under a CC-BY license.	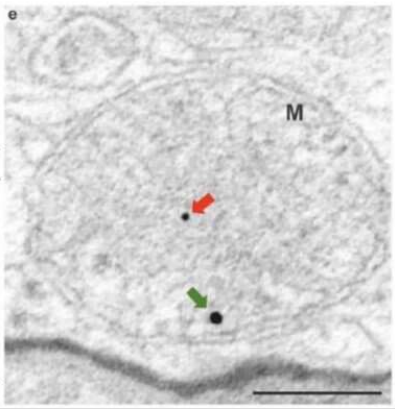

Protein content and oxidation. Gastrocnemius muscle was analyzed by immunoblotting (A) for oxidatively modified protein, STIM1, PARKIN, PINK1, PGC□1α, VDAC1, and 4HNE (B). Data are means ± SEM. *Significantly different from Tp53inp1+/+.

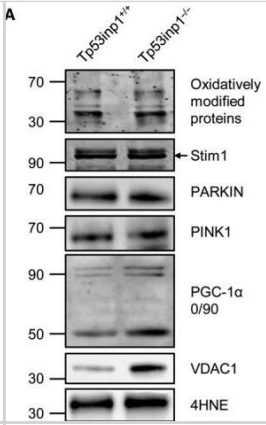

USP30 restricts basal pexophagy. H). Quantification of Keima-SKL "red" puncta in hTERT-RPE1 cells transfected with siRNA targeting USP30 (D1), PINK1 and PARKIN or non-targeting oligos (NT1). After 24 h, cells were transfected with the Keima-SKL for another 48 h prior to image capture. Average +/- SD, n = 3 independent experiments; 20 cells per experiment. One-way ANOVA and Dunnett's multiple comparison's test, **P < 0.01, overlaid on top of the data points.Summary illustration: USP30 opposes both basal pexophagy- and PINK1-dependent basal mitophagy. Image collected and cropped by CiteAb from the following publication (https://pubmed.ncbi.nlm.nih.gov/29895712), licensed under a CC-BY licence.

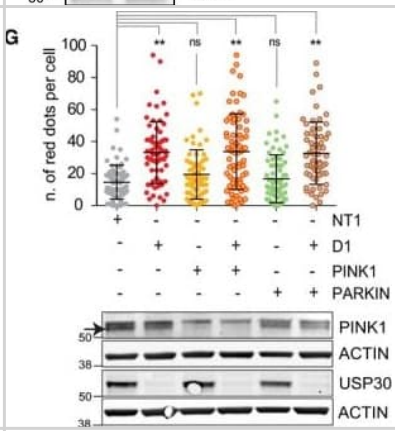

Characterisation of mitochondrial content and function in PINK1-/- platelets. (b) Cropped immunoblots showing PINK1 expression in 10 uM CCCP (6 hours) treated WT, but not KO platelets by IP (upper panel) with loading control of IP inputs by blotting for PINK1 (lower panel). Uncropped blots for PINK1 are provided in Supplementary Fig. S1b. Image collected and cropped by CiteAb from the following publication (https://pubmed.ncbi.nlm.nih.gov/30258205), licensed under a CC-BY licence.

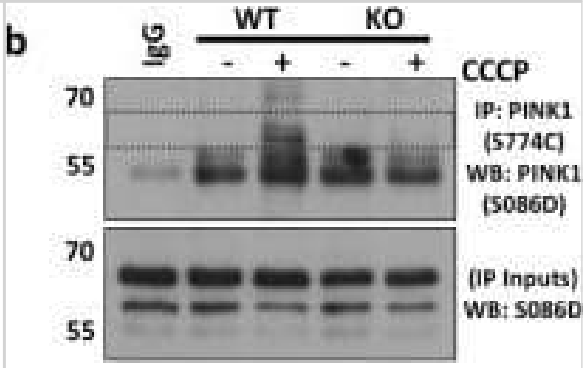

Knock-down of endogenous PINK1 abrogates Parkin Ser65 phosphorylation. (b) Knock-down of endogenous PINK1 abrogates Parkin Ser65 phosphorylation. HEK293 cells were co-transfected with PINK1 siRNA (#1 or #2) or scrambled siRNA (scrambled) and untagged wild-type (WT) or Ser65Ala (S65A) mutant Parkin as indicated using TransFectin reagent (Bio-Rad). Forty-eight hours post-transfection, cells were treated with or without 10 uM CCCP for 3 h. 0.25 mg of 1% Triton whole-cell lysate were subjected to immunoprecipitation with GST-Parkin antibody (S966C) covalently coupled to protein G Sepharose and then immunoblotted with anti-phospho-Ser65 antibody in the presence of dephosphorylated peptide. Five per cent of the IP was immunoblotted with total anti-Parkin antibody. 0.25 mg of whole-cell lysates were immunoprecipitated with anti-PINK1 antibody (S085D) and immunoblotted with anti-PINK1 antibody (Novus). Representative of three independent experiments. Image collected and cropped by CiteAb from the following publication (https://pubmed.ncbi.nlm.nih.gov/22724072), licensed under a CC-BY licence.

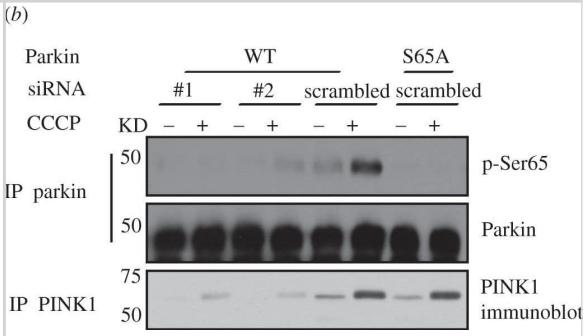

PINK1 is required for Parkin translocation but interaction between Beclin1 and Parkin is PINK1 independent. (A) HEK293T cells were transfected with scrambled siRNA and siRNA targeting SESN2 followed by treatment with 10 uM CCCP for 3 h. Total cell lysates were co-immunoprecipitated using anti-PINK1 and anti-Parkin antibodies, to find the variation in interaction between endogenous PINK1 and Parkin. Interaction of PINK1 with Parkin is less prominent on downregulation of SESN2. Image collected and cropped by CiteAb from the following publication (https://pubmed.ncbi.nlm.nih.gov/29330382), licensed under a CC-BY licence.

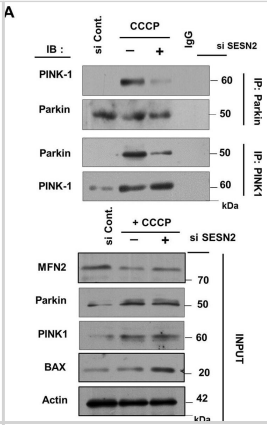

Mitophagy contributes to removal of excess mitochondrial fragments in preeclampsia. Western blot and associated densitometry of PINK1 and Parkin in PE vs. PTC mitochondrial isolates. Densitometry for PINK1 blot was used to calculate the ratio of full-length PINK63kDa to cleaved PINK153kDa (PE and PTC, n = 4 separate placentae, *P < 0.05) Image collected and cropped by CiteAb from the following publication (https://www.nature.com/articles/s41419-018-0360-0), licensed under a CC-BY licence.

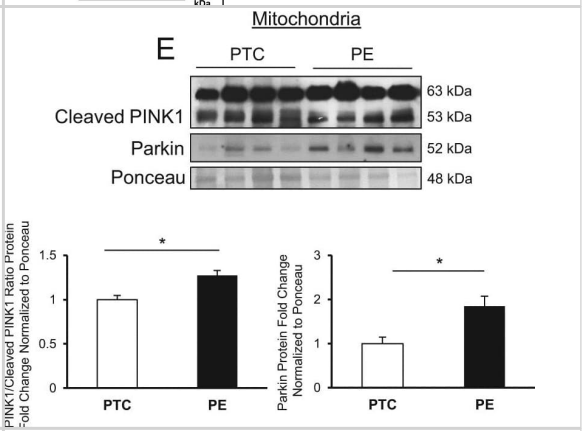

PINK1/Parkin-mediated mitophagy.D) Western Blot of mitochondrial and cytosolic fractions for PINK1, Parkin, and ubiquitin. Image collected and cropped by CiteAb from the following publication (https://pubmed.ncbi.nlm.nih.gov/33980811), licensed under a CC-BY licence.

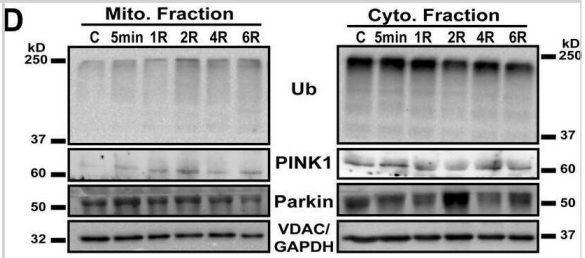

Mito-LND modulates energetic and autophagy signaling proteins in vitro and in vivo. B) Mito-LND (2 uM) modulates autophagy and specific mitophagy-linked proteins in H2030 and H2030BrM3 lung cancer cells. Image collected and cropped by CiteAb from the following publication (https://pubmed.ncbi.nlm.nih.gov/31101821), licensed under a CC-BY licence.

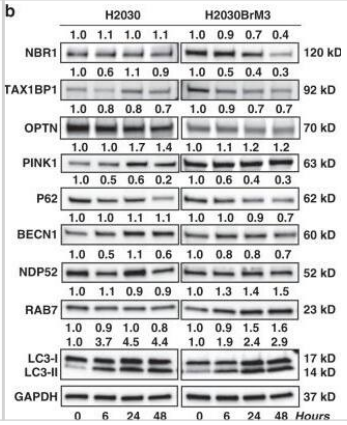

Alteration of mitochondria and PD associated proteins in SH-SY5Y cells with telomere removal by CRISPR-Cas9. (A) Representative Western blot of PGC-1alpha, NRF1, and PINK1 in SH-SY5Y cells transfected with either gTel or gCont (72 h). beta-actin served as a loading control; (B) Quantification of relative protein levels normalized to beta-actin for the indicated experimental groups (n = 3 per group); (C) Representative Western blot of parkin and AIMP2 in SH-SY5Y cells transfected with either gTel or gCont (72 h). beta-actin served as a loading control; (D) Quantification of relative protein levels normalized to beta-actin for the indicated experimental groups (n = 3 per group). Quantified data are expressed as mean +/- SEM. Statistical significance was determined by unpaired two-tailed Student's t test, * $p < 0.05$, and ** $p < 0.01$. Image collected and cropped by CiteAb from the following publication (https://www.mdpi.com/1422-0067/18/10/2093), licensed under a CC-BY licence.	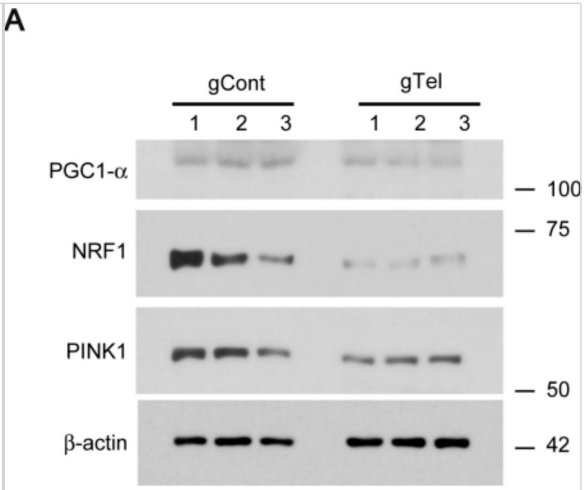
Inactivation of ATF3 potentiates PINK1 transcription. (a) Representative immunoblot analysis of ATF3 and PINK1 in total cell lysates of A549 cells, transfected with GFP (transfection control) or ATF3. Cells overexpressing ATF3 for 48 hr show lower levels of PINK1 in whole cell lysates. A549 cells transfected with siRNA scramble control or ATF3 siRNA for a total of 48 hr and exposed to tunicamycin the last 24 hr (b-d). Less ATF3 mRNA after 24 hr TM treatment (b) and a recovery of the basal PINK1 transcript levels (c) were measured in knockdown ATF3 cells. (d) At 48 hr, protein levels of ATF3 also reflect these changes after TM treatment in the presence or absence of ATF3 silencing (see Figure S2F). Data represent mean +/- SEM of four (a-c) and three (d) independent experiments. *p < .01, two-way ANOVA with multiple comparison test Image collected and cropped by CiteAb from the following publication (https://pubmed.ncbi.nlm.nih.gov/29363258), licensed under a CC-BY licence.	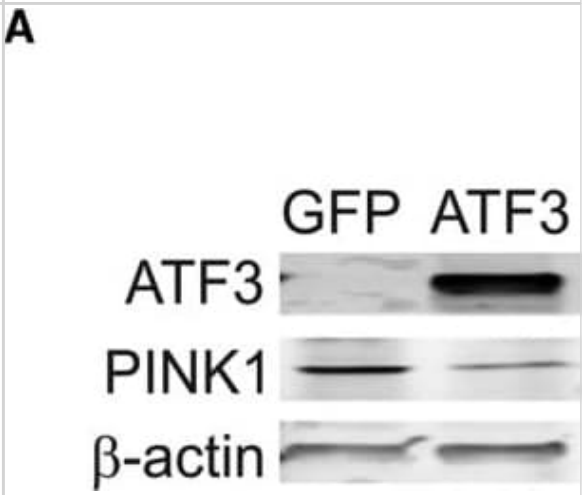
Knockdown of Pink1 inhibits mitophagy flux in CCCP-treated RPTC cells. (a) RPTC cells were subjected to: (1) control; (2) sIPC; (3) CCCP-R; (4) sIPC + CCCP-R. After treatment mitochondrial fractions were collected for immunoblot analysis of multiple mitophagy-related proteins including PINK1, PRKN, BNIP3L/NIX, FUNDC1 and DNM1L. HSPD1, a mitochondrial matrix protein, was used as a loading control. (b) RPTC cells were infected with retroviral Pink1 shRNA constructs (A-D) and a negative control (NC) construct. Upon puromycin selection, stable cells were collected for immunoblot analysis of PINK1. PPIB was used as a loading control. Based on the inhibitory effects, the stable cells (negative control, Pink1 shRNA A, Pink1 shRNA C) were transfected with COX8-EGFP-mCherry and then treated with: (1) control; (2) CCCP-R; (3) sIPC + CCCP-R. Cells were collected for fluorescence microscopy. (c) Representative images of mitolysosome formation. Scale bar: 10 um. (d) Quantitative analysis of the number of mitolysosomes per cell. Data are expressed as mean +/- SD. *, P < 0.05, significantly different from the control group; #, P < 0.05, significantly different from CCCP-R group; ^, P < 0.05, significantly different from the corresponding groups in negative control cells. Image collected and cropped by CiteAb from the following publication (https://pubmed.ncbi.nlm.nih.gov/31066324), licensed under a CC-BY licence.	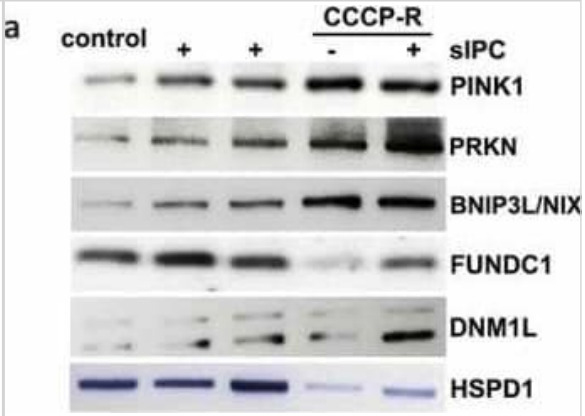

Mitophagy execution via PINK1 accumulation, MFN2/TOM20 reduction and mitophagy signaling in MDA-MB-231 cells in vitro and SST2 tumors in vivo. (D) Representative cropped PINK1 immunoblot from the mitochondrial fractions of cells treated with different MTAs for 12 hours. Bar represents the mean +/- SEM. (n=4). Image collected and cropped by CiteAb from the following publication (https://www.oncotarget.com/lookup/doi/10.18632/oncotarget.23171), licensed under a CC-BY licence.	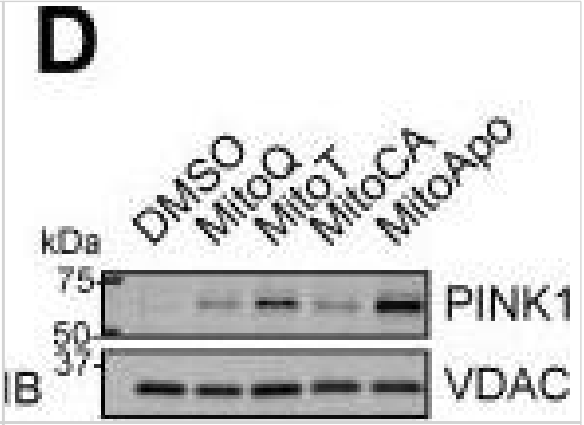
PINK1 and Parkin are phosphorylated after a decrease in deltapsim in mouse primary neurons. Neurons were infected with lentivirus encoding PINK1-Flag (A), wild-type HA-Parkin (B) or HA-Parkin with either the S65A or S65E mutation (C). Cells were treated with the mitochondrial uncoupler CCCP (30 um) for 1-3 h and subjected to SDS-PAGE in the absence or presence of 50 um phos-tag. Note that mobility does not reflect the molecular weight of proteins in phos-tag PAGE (Kinoshita et al. 15), and thus, molecular weight markers are not shown in the bottom gels. The red and black asterisks in (C) indicate phosphorylation of Parkin at Ser65 and an additional minor phosphorylation site, respectively. Image collected and cropped by CiteAb from the following publication (https://pubmed.ncbi.nlm.nih.gov/23751051), licensed under a CC-BY licence.	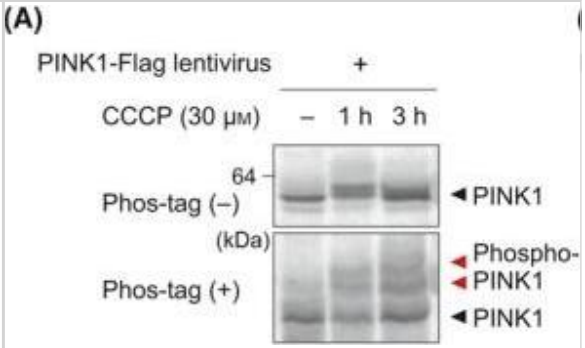
PPM1H does not dephosphorylate Ser111 of Rab8A or key phosphorylation sites of AMPK and Akt signaling pathways.(A) HEK293 cells were transiently transfected with constructs expressing the indicated components. 24 hr post-transfection, cells were treated +/-10 uM CCCP (Carbonyl cyanide m-chlorophenyl hydrazine) for 3 hr to induce activation of the PINK1 kinase and trigger Rab8A phosphorylation at Ser111 (Lai et al., 2015). (B) As in (A) except cells were immunoblotted with the indicated antibodies that recognize key phosphorylation sites of AMPK and Akt signaling pathways. Image collected and cropped by CiteAb from the following publication (https://pubmed.ncbi.nlm.nih.gov/31663853), licensed under a CC-BY licence.	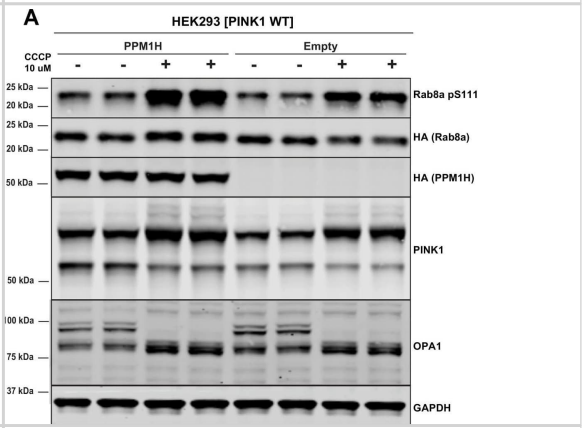
Representative immunohistochemical expression for HIF-1α, c-Met, CA9 and GLUT1. HIF-1α is stained in cytoplasm shown with no staining in normal cervix (A), weak staining intensity in high grade CIN (B), and strong staining intensity in squamous cell carcinoma (C). c-Met (D-F), CA9 (G, H) and GLUT1 (I) shows cell membranous staining. Representative c-Met expression in cervical samples shown with no staining in normal cervix (D), weak membranous staining intensity in squamous cell carcinoma (E) and strong intensity in squamous cell carcinoma (F). CA9 expression showing moderate intensity staining in carcinoma in situ (CIS) (G) and strong staining in adenocarcinoma (H). GLUT1 expression showing strong intensity in squamous cell carcinoma (I). Scale bar: 50 μm. Image collected and cropped by CiteAb from the following open publication (https://translational-medicine.biomedcentral.com/articles/10.1186/1479-5876-11-185), licensed under a CC-BY license. Not internally tested by Novus Biologicals.	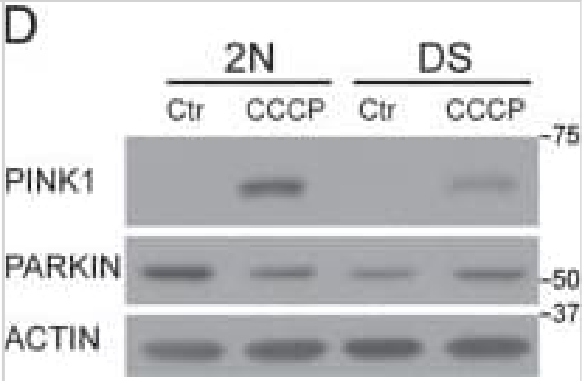

Effect of PGE1 on stability and synthesis of HIF-1α.(A) Human aortic smooth muscle cells (HASMCs) and human umbilical vein endothelial cells (HUVECs) were exposed to 1 μM PGE1 or 100 μM DFX or incubated for 4 h, and CHX was added to a final concentration of 100 μM. The cells were incubated for 0 to 30 min, and whole-cell lysates were subjected to immunoblot assay using anti-HIF-1α or -β antibodies. (B) Serum-starved HASMCs were pretreated with no drug and 1 μM PGE1 for 30 min in Met-free medium. [35S]Met-Cys was added, and the cells were incubated for 60 min prior to preparation of cell lysates. Aliquots of 1 mg of the lysates were subjected to immunoprecipitation with anti-HIF-1α antibody, separated by SDS-PAGE and exposed. Aliquots of 50 μg of the same lysate were separately subjected to immunoblotting analysis with anti-β-actin antibody. (C) HASMCs and HUVECs were exposed to vehicle or 1 μM PGE1 for 4 h in the presence of 10 μM LY294002 (LY), 50 μM PD98059 (PD), or 5 μM GF109203X (GF). The cells were harvested and the whole-cell lysates were subjected to immunoblot assay for HIF-1α and β-actin protein expression. Experiments were repeated at least twice. Representative immunoblots are shown. (D) HASMCs were exposed to vehicle or 1 μM PGE1 for 12 h in the presence of 10 μM LY294002 (LY), 50 μM PD98059 (PD), or 5 μM GF109203X (GF). Cells were harvested and subjected to semi-quantitative RT-PCR for VEGF and GLUT1. Experiments were repeated three times. Fold induction relative to that under 20% O2 without PGE1 treatment was plotted. □P < 0.05 compared with the control (20%, PGE1 treatment without any kinase inhibitors). Image collected and cropped by CiteAb from the following open publication (https://pubmed.ncbi.nlm.nih.gov/24349900), licensed under a CC-BY license. Not internally tested by Novus Biologicals.

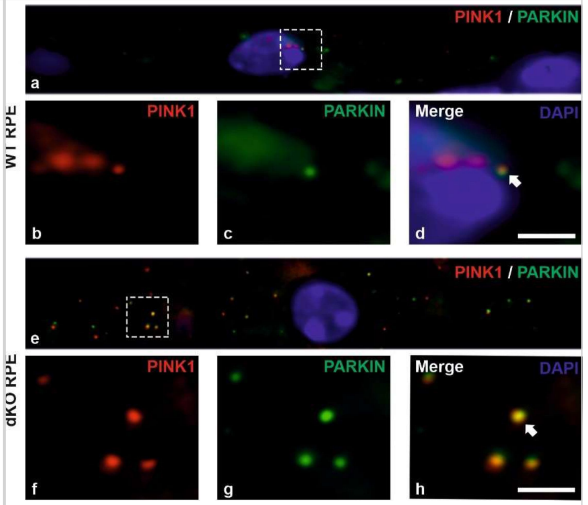

Expression of PRDX2 or PRDX4 does not affect HIF-1α or HIF-2α protein levelsA. and B. HeLa cells were transfected with EV or vector encoding PRDX2-V5 (A, P2) or PRDX4-V5 (B, P4), and exposed to 20% or 1% O2 for 24 h. WCL was subject to immunoblot assays with antibody against HIF-1α, HIF-2α, V5, or acin. C. HeLa-shSC (sc) and HeLa-shPRDX(2+4) (2+4) cells were exposed to 20% or 1% O2 for 24 h in the presence of doxycycline. WCL was subject to immunoblot assays with antibodies against HIF-1α, HIF-2α, PRDX2, PRDX4, and actin. Image collected and cropped by CiteAb from the following open publication (https://www.oncotarget.com/lookup/doi/10.18632/oncotarget.7142), licensed under a CC-BY license. Not internally tested by Novus Biologicals.

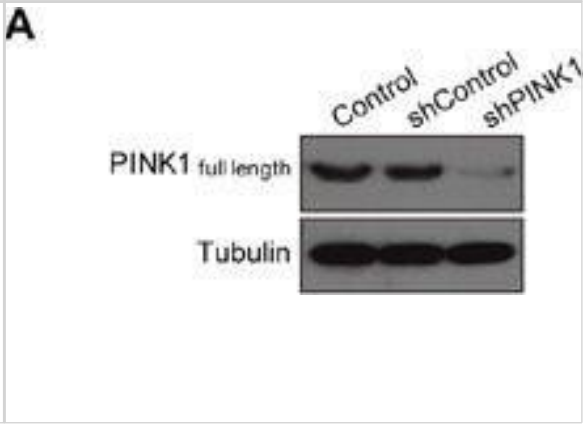

Spontaneously metastasizing tumor cells survive significantly longer at the secondary site compared to intravenously injected tumor cells.a Representative intravital microscopy images showing the possible fates of extravascular disseminated tumor cells in the lung parenchyma. Top: Images of disseminated tumor cells just after extravasation. Bottom left: Example of an extravascular tumor cell, which has died, as evidenced by small extravascular apoptotic bodies (yellow arrow). Bottom middle: Example of an extravascular tumor cell that survived as a single and solitary tumor cell over time. Bottom right: Example of an extravascular tumor cell that began to divide and grow into a micro-metastasis. Red = tdTomato labeled endothelial cells and 155 kDa Tetramethylrhodamine dextran labeled blood serum, Green = GFP labeled tumor cells. Yellow dashed lines delineate blood vessel boundaries. Scale bar = 15 μm. b Percentage of extravascular E0771-GFP disseminated tumor cells that died, survived, or grew after extravasation in EM and SM models 64 hrs after arrival to the lung vasculature. EM: n = 27 tumor cells in 4 mice. SM: n = 31 tumor cells in 4 mice. Bar = mean. Error bars = ±SEM. For Died and Survived columns, a two-tailed unpaired t-test was used (p = 0.0003 and 0.0005, respectively). For Grew columns, a two-tailed Mann-Whitney test was used (p = 0.14). ***p < 0.001. ns = not significant. Source data are provided as a Source Data file. Image collected and cropped by CiteAb from the following open publication (https://pubmed.ncbi.nlm.nih.gov/35110548), licensed under a CC-BY license. Not internally tested by Novus Biologicals.

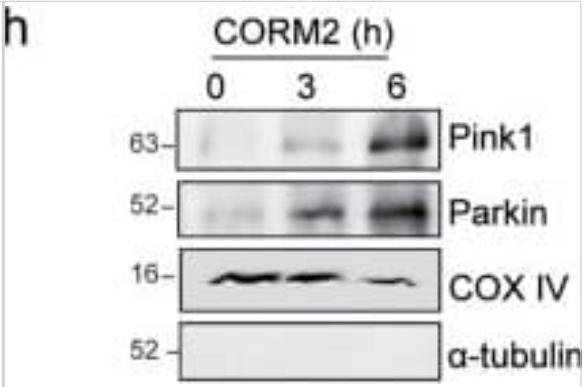

Functional assessment of Fanconi anemia pathway. (a) The experimental scheme for MMC treatment. Twenty□four hours after plating, cells were cultured with or without MMC 1 μM for an additional 24 hr, after which the cells were harvested for western blot or immunostaining. (b) Western blot with FANCD2 antibody of BJ, proband fibroblasts, FANCB mutant (null) fibroblasts and FANCD2 mutant (null) fibroblasts. (c) Western blot with FANCD2 antibody of non□FA control lymphoblasts (LCL), proband LCL□A□2017, proband LCL□B□2017, FANCB mutant (null) LCL, and FANCD2 mutant (null) LCL. (d) Representative figures of FANCD2 foci formation in the indicated cells. (e) Quantification of FANCD2 foci formation following treatment with or without 1 μM MMC. Experiments were performed in triplicate. One hundred cells were counted for each experiment Image collected and cropped by CiteAb from the following open publication (https://pubmed.ncbi.nlm.nih.gov/29193904), licensed under a CC-BY license. Not internally tested by Novus Biologicals.

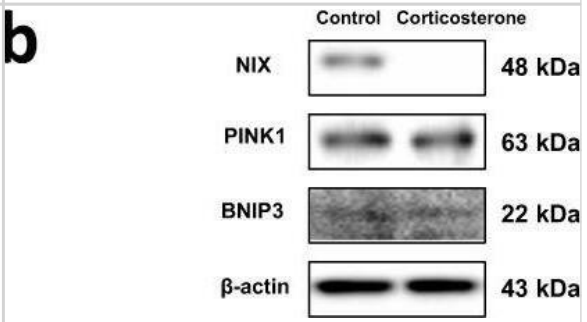

Detailed schematic and validation of the FKBP5 TRE transgene. A, To allow for site-directed, single copy insertion into the mouse genome in chromosome 11, the transgenic construct contained flanking attB sites via a PhiC31 integrase. The downstream Mp1 poly A tail will help maintain stable expression. To drive high expression, the transgenic construct included a tetracycline-response element (TRE) promoter made of seven repeats of the tetracycline operators used to drive high expression of the singly inserted FKBP5 gene in the presence of the tTA, and a weak minimal CMV promoter which produces low basal expression. B, Western blotting from HEK293T cells transfected with increasing amounts of FKBP5 TRE plasmid, as indicated, for 48 h. C, HEK293T cells were transfected with the indicated amounts of FKBP5 TRE and tTA plasmid, to ensure the tTA would drive high FKBP51 expression. Image collected and cropped by CiteAb from the following open publication (https://pubmed.ncbi.nlm.nih.gov/30963102), licensed under a CC-BY license. Not internally tested by Novus Biologicals.

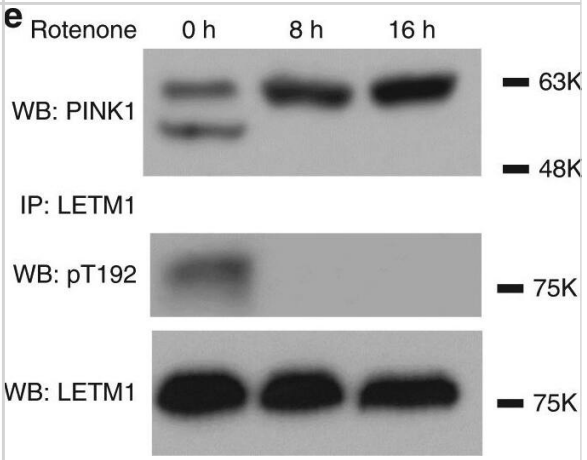

Truncated Sin1 displaces endogenous Sin1 from mTORC2 in DLD1 colon cancer cellsA. Schematic indicating the domain structure of Sin1 and the constructs used to displace endogenous Sin1 from mTORC2. B. Expression of myc tagged Sin1 constructs can be detected only after induction with Doxycycline (Dox). Cells were treated with 100nM of doxycycline (+) for 72 hours and expressed proteins were detected by immunoblot of whole cell lysates with anti-myc (9E10) antibodies. C. and D. Sin1 constructs incorporate into mTORC2 and displace endogenous Sin1. Constructs were induced for 72 hours prior to immune precipitation. (C) mTORC2 subunits, mTOR and Rictor, only appear in myc immunoprecipitates after induction with doxycycline (Left panels); myc-ΔSin1 cannot be directly detected in precipitates due to secondary antibody cross reaction with precipitating IgG. Right panels indicate unchanging expression levels of Rictor and mTOR in immune precipitation input lysates, which is further quantified from 3 independent experiments E. Endogenous Sin1 and Rictor immunoprecipitates demonstrate displacement of endogenous Sin1 from mTORC2. Following induction, band shifted myc-tagged FL Sin1 can be detected in Sin1 and Rictor precipitates (Left panels). Truncated ΔSin1 can be detected in Rictor, but not Sin1, immunoprecipitates as the Sin1 antibody epitope is deleted from ΔSin1. F. Quantification of Sin1 levels detected in Rictor immunoprecipitates indicates the level of endogenous mTORC2 disruption following Sin1 construct induction (data are mean +/- S.D; n = 3). Myc-ΔSin1 displaces >80% of endogenous Sin1 while levels of myc-FL Sin1 associated with Rictor are comparable with endogenous Sin1 levels. Image collected and cropped by CiteAb from the following open publication (https://www.oncotarget.com/lookup/doi/10.18632/oncotarget.20086), licensed under a CC-BY license. Not internally tested by Novus Biologicals.

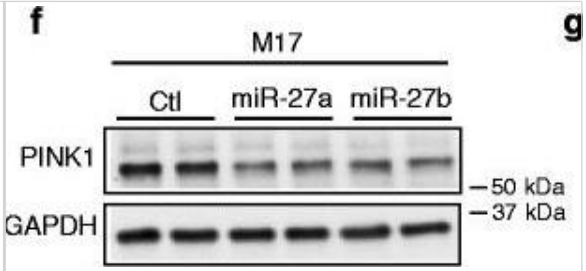

The FANCD2 NLS is required for efficient FANCD2 and FANCI monoubiquitination and chromatin association.(A) FA-D2 cells stably expressing LacZ, FANCD2-WT, FANCD2-K561R, FANCD2-ΔN57, FANCD2-ΔN100 and FANCD2-3N were incubated in the absence and presence of 250 nM MMC for 18 h, and whole-cell lysates were immunoblotted with antibodies to FANCD2, V5, FANCI and α-tubulin. The FANCD2 and FANCI L/S ratios are the ratios of monoubiquitinated to nonubiquitinated protein, and were calculated by measuring protein band intensities using ImageJ image processing and analysis software (https://rsb.info.nih.gov/ij/). (B and C) FA-D2 cells stably expressing FANCD2-WT, FANCD2-ΔN57, FANCD2-ΔN100 and FANCD2-3N were treated as above and cell pellets were fractionated into soluble (S) and chromatin-associated (C) fractions. Fractions were immunoblotted with antibodies against V5, FANCI, α-tubulin and H2A. W, unfractionated whole cell extract. Image collected and cropped by CiteAb from the following open publication (https://pubmed.ncbi.nlm.nih.gov/24278431), licensed under a CC-BY license. Not internally tested by Novus Biologicals.

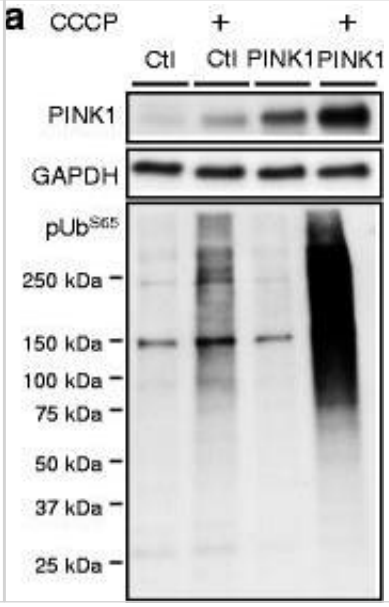

Immunoblot analyses of protein expression for Nrf2 and antioxidant enzymes.A. Analysis of nuclear Nrf2 in young and old mice subjected to EES. In sedentary mice, Nrf2 protein levels were decreased significantly in young versus old mice. EES exacerbated the decrease of nuclear Nrf2 in old mice. Blots/values represent n=4–6 from each group. *p<0.05 between young vs. old and #p<0.05-between basal vs. EES. (B) Representative immunoblots of cytosolic extracts from the hearts of young and old mice under basal conditions and following EES. Protein blots were probed with anti-HO1, NQO1, GCLM, GCLC, Catalase, SOD1, SOD2, GSR, G6PD, GPX1 and GAPDH. Individual lanes indicate a single animal. Densitometry analysis of respective protein signals was performed using Image-J and expressed as relative intensity units calculated as mean values of young and old, *p<0.05. Individual lanes indicate each animal (n=6). #p<0.05-between basal and EES. Image collected and cropped by CiteAb from the following open publication (https://dx.plos.org/10.1371/journal.pone.0045697), licensed under a CC-BY license. Not internally tested by Novus Biologicals.

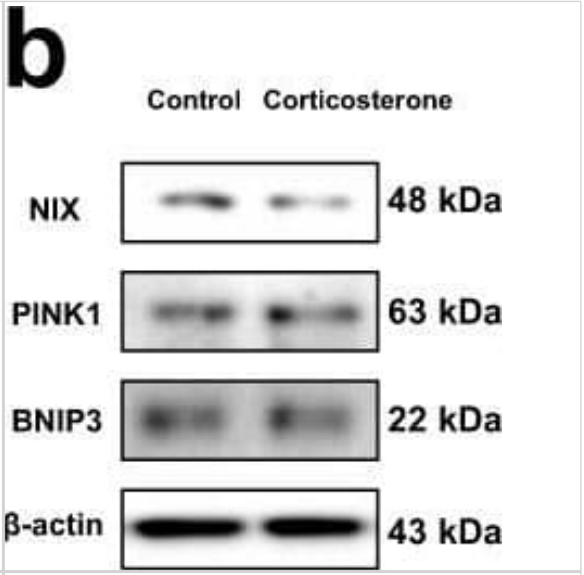

Optn or p62 deficiency affects autophagosome formation.(A) Workflow of the experiments shown in (B-G). Larvae were treated with 100 nM of Baf A1 for 12 h from 3.5 dpf. The GPF-Lc3 negative larvae were selected to assay autophagy activity by Western blot, the GFP-Lc3 positive larvae were collected to monitor autophagic activity using confocal imaging. The red square indicates the region for confocal imaging. (B) Level of basal autophagy in WT and mutant embryos in absence or presence of Baf A1. Protein samples were extracted from 4 dpf WT and mutant larvae (>10 embryos/sample). The blots were probed with antibodies against Lc3 and Actin as a loading control. Western blots were repeated at least three times with independent extracts. (C) Quantification of Lc3-II fold changes in WT and mutant embryos in absence or presence of Baf A1. Western blot band intensities were quantified by Lab Image. Data is combined from three independent experiments. (D) Representative confocal micrographs of GFP-Lc3 puncta present in the tail fin of optn+/+, optnΔ5n/Δ5n, p62+/+ and p62Δ37n/Δ37n at 4 dpf. Scale bars, 10 μm. (E). Quantification of the number of GFP-Lc3 puncta in optn+/+, optnΔ5n/Δ5n, p62+/+ and p62Δ37n/Δ37n larvae with and without Baf A1 treatment. Each larva was imaged at a pre-defined region of the tail fin (as indicated by the red boxed area in Fig3 A) (≥11 larvae/group). Results are accumulated from two independent experiments. ns, non-significant, *p<0.05, **p<0.01, ***p<0.001. Image collected and cropped by CiteAb from the following open publication (https://pubmed.ncbi.nlm.nih.gov/30818338), licensed under a CC-BY license. Not internally tested by Novus Biologicals.

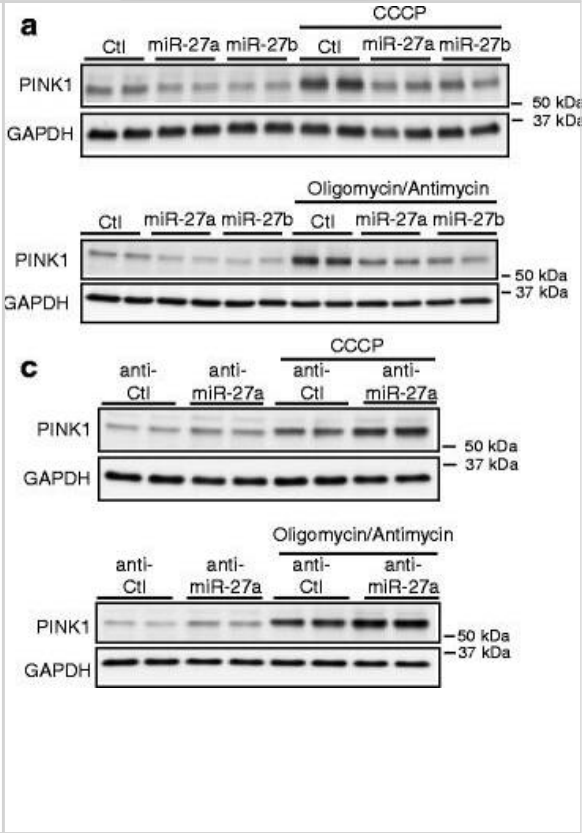

Increased expression of HIFα and/or Twist in A549 and H441 cells induced by the inhibition of PIMT and Thapsigargin(A) Immunoblotting of Slug, ZEB1, Snail1, Twist, and HIF1α in A549 sh-PIMT and sh-control cells. (B, C) Immunoblotting and relative intensity of HIF1α in A549 cells treated with Tg. (D) Immunoblotting of Slug, ZEB1, Snail1, Twist, and HIF1α in si-control cells and si-PIMT H441 cells. (E, F) Immunoblotting and relative intensity of HIF1α in H441 cells treated with Tg. #1 and #2 indicates si-RNA of J-010000-05-0002 and J-010000-07-0002, respectively. Image collected and cropped by CiteAb from the following open publication (https://www.oncotarget.com/lookup/doi/10.18632/oncotarget.24324), licensed under a CC-BY license. Not internally tested by Novus Biologicals.

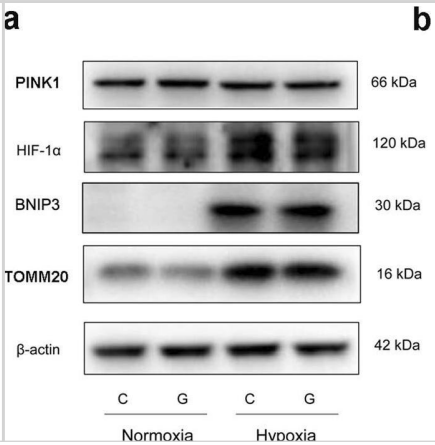

Flow cytometry gating strategy for quantification of platelet-derived microparticles in equine platelet samples.A: Platelet events in citrate-anticoagulated platelet-rich plasma were identified and gated as CD41-positive cells (R1 region) in a CD41 fluorescence versus forward scatter (FSC) dotplot. The R1 region or gate was established on an isotype control for the CD41 antibody. Representative image from platelets exposed to the RacL11 strain of EHV-1 at 1 plaque forming unit (PFU)/cell. B: Platelet-derived microparticles (PDMPs) were defined as small events (<101 log FSC units) positive for Annexin V and CD41. The PDMP percentage was obtained from the lower right quadrant of an Annexin V fluorescence versus FSC dotplot of the R1 gate (CD41-positive events), with the quadrants being defined on a negative sample in which 1 mM EDTA was added to the buffer with Annexin V. The PDMP percentage was 0.1% in this representative image of platelets exposed to rabbit kidney 13 (RK) cell lysate at an equivalent volume to 1 PFU/cell (mock-infected negative control). The events in the upper left and right quadrants are platelets that are negative (94.0%) and positive for Annexin V (0.9%), respectively. C: Representative image of PDMP quantification in platelets exposed to RacL11 at 1 PFU/cell. In this sample, there are 12.1% PDMP (lower right quadrant) and 22.1% of platelets are weakly positive for Annexin V (upper right quadrant). Image collected and cropped by CiteAb from the following open publication (https://pubmed.ncbi.nlm.nih.gov/25905776), licensed under a CC-BY license. Not internally tested by Novus Biologicals.

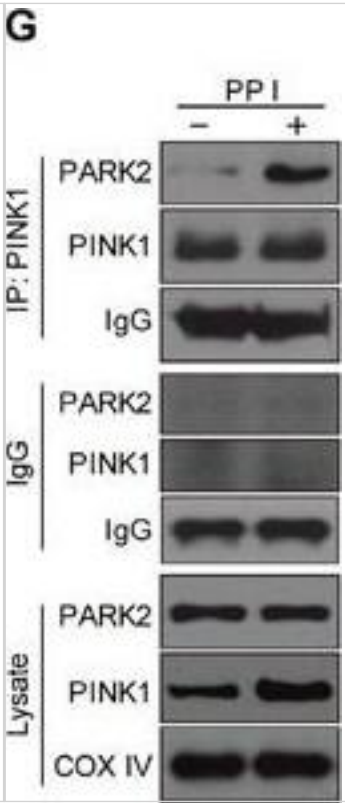

Inhibition of MST improves liver regeneration in aged miceAged mice (> 12 months) were injected i.v. with siScr or siMST. Twenty□four hours after siRNA injection, a 70% PH was performed and remnant/regenerating liver tissue was harvested 40 h later. p.i. of the livers was calculated by IHC staining of Ki67□positive hepatocytes and livers were classified as (−) non□regenerating or (+) regenerating based on the percentage of positive cells. Non□surviving animals were sacrificed before the 40□h end time point. “n” indicates the number of animals per group.Ki67 immunostaining of the regenerating aged mice livers, 40 h post□PH. Sections were scanned using 3DHistech Pannoramic MIDI Scanner and quantitated with Quant Center 2.0 software. p.i. values are provided on the image.Representative photomicrograph of an aged liver treated with siMST and stained with H&E and by IHC for CK19 and Ki67. Arrows indicate ductal regions with no signs of reaction or oval cell expansion.Quantitative RT–PCR analysis of RNA isolated from mouse liver for Foxm1B, Birc5 and Ccnb1 at 0 and 40 h post□PH. Log2 fold change was calculated using non□transfected/non□resected mouse liver as a control. Representative results from a single experiment with n = 6 animals per group are shown. Paired, two□tailed Student's t□test was used to calculate the significant change in signals between liver tissues at the time of resection (0 h) compared to 40 h post□PH.Percentage of Ki67□positive hepatocytes in aged and aged + siMST 40 h post□resection. Representative results from a single experiment with n = 6 independent aged animals for group are shown. Two□tailed Student's t□test was used to calculate the significance of percentage of positive hepatocytes of siMST□treated animals compared to non□treated controls.Endpoint liver weight was taken of the remnant lobe and expressed as a percentage to total body weight. Representative results from a single experiment with n = 6 independent animals for group expect for control group where n = 6 are shown. Estimated liver□to□body weight ratio before PH in mice = 3.85 ± 0.05 (SD). Unpaired, two□tailed Student's t□test was used to calculate the significance of each aged group in comparison with the control young group.Hepatocyte geometric diameter was determined (see Materials and Methods). Representative results from a single experiment with n = 3 independent animals per group. Unpaired, two□tailed Student's t□test was used to calculate the significant change in hepatocyte size in liver tissue with and without siMST 40 h post□PH.Data information: Bars represent mean ± SD. Scale bars, 50 μm. Image collected and cropped by CiteAb from the following open publication (https://pubmed.ncbi.nlm.nih.gov/27940445), licensed under a CC-BY license. Not internally tested by Novus Biologicals.

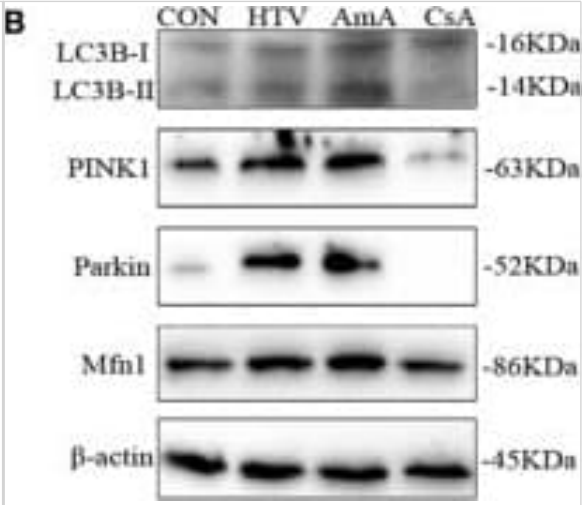

Publications

George F G Allen, Rachel Toth, John James, Ian G Ganley Loss of iron triggers PINK1/Parkin-independent mitophagy EMBO Reports 2013-12-01 [PMID: 24176932]

Seo Jeong Jeon, Kwang Chul Chung The SCF-FBW7β E3 ligase mediates ubiquitination and degradation of the serine/threonine protein kinase PINK1 The Journal of Biological Chemistry 2024-03-18 [PMID: 38508312]

Inge Kinnart, Liselot Manders, Thibaut Heyninck, Dorien Imberechts, Roman Praschberger, Nils Schoovaerts, Catherine Verfaillie, Patrik Verstreken, Wim Vandenberghe Elevated α-synuclein levels inhibit mitophagic flux NPJ Parkinson's Disease 2024-04-09 [PMID: 38594264]

Jie Tang, Xiaoxue Lu, Tao Zhang, Yuyang Feng, Qiaolin Xu, Jing Li, Yuanzhi Lan, Huaxing Luo, Linghai Zeng, Yuanyuan Xiang, Yan Zhang, Qian Li, Xuhu Mao, Bin Tang, Dongzhu Zeng Shiga toxin 2 A-subunit induces mitochondrial damage, mitophagy and apoptosis via the interaction of Tom20 in Caco-2 cells Heliyon 2023-09-09 [PMID: 37809632]

Karan Sharma, Asha Kishore, Anna Lechado-Terradas, Raffaele Passannanti, Francesco Raimondi, Marc Sturm, Ashwin Ashok Kumar Sreelatha, Divya Kalikavila Puthenveedu, Gangadhara Sarma, Nicolas Casadei, Rejko Krüger, Thomas Gasser, Philipp Kahle, Olaf Riess, Julia C Fitzgerald, Manu Sharma A Novel PINK1 p.F385S Loss-of-Function Mutation in an Indian Family with Parkinson's Disease. Movement disorders : official journal of the Movement Disorder Society 2024-04-08 [PMID: 38586902]

Wenting You, Kèvin Knoops, Tos T. J. M. Berendschot, Birke J. Benedikter, Carroll A. B. Webers, Chris P. M. Reutelingsperger, Theo G. M. F. Gorgels PGC-1a mediated mitochondrial biogenesis promotes recovery and survival of neuronal cells from cellular degeneration Cell Death Discovery 2024-04-17 [PMID: 38632223]

Wauters, F;Cornelissen, T;Imberechts, D;Martin, S;Koentjoro, B;Sue, C;Vangheluwe, P;Vandenberghe, W; LRRK2 mutations impair depolarization-induced mitophagy through inhibition of mitochondrial accumulation of RAB10 Autophagy 2019-04-04 [PMID: 30945962]

Iswariyaraja Sridevi Gurubaran Mitochondrial damage and clearance in retinal pigment epithelial cells. Acta ophthalmologica 2024-03-13 [PMID: 38467968]

Laura Jankó, Tünde Kovács, Miklós Laczik, Zsanett Sári, Gyula Ujlaki, Gréta Kis, Ibolya Horváth, Miklós Antal, László Vígh, Bálint L. Bálint, Karen Uray, Péter Bai, Ted M. Dawson, Oleh Khalimonchuk Silencing of Poly(ADP-Ribose) Polymerase-2 Induces Mitochondrial Reactive Species Production and Mitochondrial Fragmentation Cells 2021-06-04 [PMID: 34199944]

Christy B. M. Tulen, Ying Wang, Daan Beentjes, Phyllis J. J. Jessen, Dennis K. Ninaber, Niki L. Reynaert, Frederik-Jan van Schooten, Antoon Opperhuizen, Pieter S. Hiemstra, Alexander H. V. Remels Dysregulated mitochondrial metabolism upon cigarette smoke exposure in various human bronchial epithelial cell models Disease Models & Mechanisms 2022-03-01 [PMID: 35344036]

J. Tabitha Hees, Simone Wanderoy, Jana Lindner, Marlena Helms, Hariharan Murali Mahadevan, Angelika B. Harbauer Insulin signalling regulates Pink1 mRNA localization via modulation of AMPK activity to support PINK1 function in neurons Nature Metabolism 2024-03-19 [PMID: 38504131]

Stephanie B Levy, Richard G Bribiescas Hierarchies in the energy budget: Thyroid hormones and the evolution of human life history patterns. Evolutionary anthropology 2023-10-01 [PMID: 37584402]

More publications at http://www.novusbio.com/BC100-494

Procedures

Western Blot protocol for PINK1 Antibody (BC100-494)

Western Blot Protocol

1. Perform SDS-PAGE on samples to be analyzed, loading 10-25 ug of total protein per lane.
2. Transfer proteins to PVDF membrane according to the instructions provided by the manufacturer of the membrane and transfer apparatus.
3. Stain according to standard Ponceau S procedure (or similar product) to assess transfer success, and mark molecular weight standards where appropriate.
4. Rinse the blot of the protein stain.
5. Block the membrane using 5% BSA for at least 1 hour.
6. Dilute anti-PINK1 primary antibody in 1-5% w/v BSA in TBS with 0.1% Tween-20 for 1 hour at room temperature.
7. Wash the membrane in wash buffer three times for 10 minutes each.
8. Incubate in diluted HRP-conjugated Rabbit secondary antibody in 1% BSA (as per manufacturers instructions) and incubate 1 hour at room temperature.
9. Wash the blot in wash buffer three times for 10 minutes each (this step can be repeated as required to reduce background).
10. Apply the detection reagent of choice in accordance with the manufacturers instructions.

Novus Biologicals USA
10730 E. Briarwood Avenue
Centennial, CO 80112
USA
Phone: 303.730.1950
Toll Free: 1.888.506.6887
Fax: 303.730.1966
nb-customerservice@bio-techne.com

Bio-Techne Canada
21 Canmotor Ave
Toronto, ON M8Z 4E6
Canada
Phone: 905.827.6400
Toll Free: 855.668.8722
Fax: 905.827.6402
canada.inquires@bio-techne.com

Bio-Techne Ltd
19 Barton Lane
Abingdon Science Park
Abingdon, OX14 3NB, United Kingdom
Phone: (44) (0) 1235 529449
Free Phone: 0800 37 34 15
Fax: (44) (0) 1235 533420
info.EMEA@bio-techne.com

General Contact Information
www.novusbio.com
Technical Support: nb-technical@bio-techne.com
Orders: nb-customerservice@bio-techne.com
General: novus@novusbio.com

Limitations
This product is for research use only and is not approved for use in humans or in clinical diagnosis. Primary Antibodies are guaranteed for 1 year from date of receipt.

For more information on our 100% guarantee, please visit www.novusbio.com/guarantee

Earn gift cards/discounts by submitting a review: www.novusbio.com/reviews/submit/BC100-494

Earn gift cards/discounts by submitting a publication using this product: www.novusbio.com/publications